

Role of GTP Hydrolysis in Fission of Caveolae Directly from Plasma Membranes

Jan E. Schnitzer,* Phil Oh, Deirdre P. McIntosh

Caveolae are specialized invaginated cell surface microdomains of undefined function. A cell-free system that reconstituted fission of caveolae from lung endothelial plasma membranes was developed. Addition of cytosol and the hydrolysis of guanosine triphosphate (GTP) induced caveolar fission. The budded caveolae were isolated as vesicles rich in caveolin and the sialoglycolipid G_{M1} but not glycosyl-phosphatidylinositol (GPI)-anchored proteins. These vesicles contained the molecular machinery for endocytosis and transcytosis. In permeabilized endothelial cells, GTP stimulated, whereas $GTP\gamma S$ prevented, caveolar budding and endocytosis of the cholera toxin B chain to endosomes. Thus, caveolae may bud to form discrete carrier vesicles that participate in membrane trafficking.

Transport studies in many cell types using various tracers detectable by electron microscopy suggest a role for caveolae in transcytosis, endocytosis, or both (1–5). Specific binding molecules have been identified (1, 6–9), as well as various possible inhibitors or stimulators of apparent transport mediated by caveolae (4, 5, 10). Although select labeling within caveolae has been interpreted as indicative of transport by caveolae (1–5, 7), such ultrastructural studies can neither prove that caveolae function in transport nor ascertain whether they do so by budding to form discrete carrier vesicles capable of targeted delivery (11). Because of the racemose structure of caveolae, wherein vesicles are linked to form a grape-like branching “cave” penetrating deep into the cell, conventional sections for electron microscopy misleadingly show about 50% of the vesicles apparently free in the cytoplasm, whereas serial ultrathin sectioning reveals that only 1% or less are truly free and unattached to other membranes (11, 12). Thus, some investigators have concluded that caveolae, even in endothelium, are not dynamic but rather fixed permanent invaginations incapable of budding (11–13). In the midst of this controversy, potocytosis was proposed as an alternative mechanism for the movement of small molecules directly into cells without the need for caveolar internalization (13).

To develop a molecular approach to studying caveolae, we recently have shown that luminal endothelial cell plasma membranes selectively coated in situ by vascular perfusion of colloidal silica particles can be purified from rat lungs and that their caveolae can be separated from these membranes by stringent shearing during homogenization and then purified to homogeneity by density centrifuga-

tion (14). If caveolae can bud from the cell surface to transport their cargo, it may be possible to release caveolae from plasma membranes under more physiological conditions by reconstituting the intracellular environment.

We found that in the presence of cytosol (15), the addition of guanosine triphosphate (GTP) stimulated the release of caveolae from the purified silica-coated plasma membranes in the absence of any homogenization (16). Caveolin was released from these membranes in a concentration- and time-dependent manner (Fig. 1). A maximal response was achieved in 60 min with 1 mM GTP, with an apparent median effective dose of 30 μM (Fig. 1C). Only $20 \pm 5.7\%$ of the caveolin remained associated with the plasma membrane fraction after GTP treatment ($n = 3$). By contrast, the signal for other plasmalemmal marker proteins not present in caveolae, such as angiotensin-converting enzyme (ACE) and the glycosyl-phosphatidylinositol (GPI)-anchored protein 5'-nucleotidase (5'NT), remained constant (Fig. 1, A and B). The GTP concentration significantly affected the kinetics of caveolar budding, with a maximum rate at 1 mM GTP giving a half-life for budding of 10 min (Fig. 2A). Caveolar fission specifically required GTP hydrolysis because adenosine 5'-triphosphate (ATP), uridine 5'-triphosphate (UTP), cytidine 5'-triphosphate (CTP), GDP β S, and the nonhydrolyzable GTP analog $GTP\gamma S$ did not induce fission (Fig. 2B). In fact, $GTP\gamma S$ competitively inhibited the GTP-induced fission of caveolae (Fig. 2C).

As shown for caveolae physically removed from the silica-coated plasma membranes (14), the caveolin-rich vesicles released by GTP hydrolysis could be isolated by sucrose gradient centrifugation as a low-density membrane fraction well separated from the plasma membranes (Fig. 3A). With GTP but not $GTP\gamma S$ treatment, caveolin was detected in fractions 5 to 10 of

the sucrose gradient.

The isolated GTP-released free caveolar vesicles contained several molecules associated with various aspects of transport (Fig. 3B). The vesicles were rich in G_{M1} , a receptor for the endocytosis of cholera toxin B chain (CTB) (1). In addition, the vesicle-docking

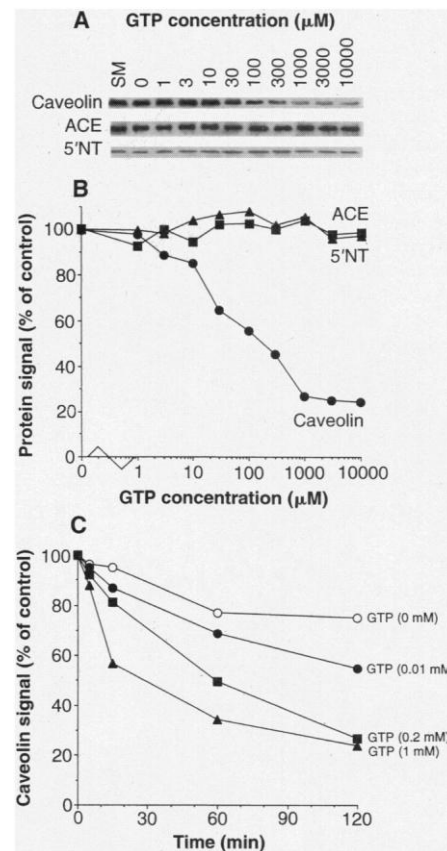


Fig. 1. GTP-stimulated release of caveolin but not other noncaveolar proteins from plasma membranes. **(A)** The luminal endothelial cell plasma membranes of rat lungs were coated in situ with a colloidal silica solution and purified from tissue homogenates (14). These silica-coated endothelial plasma membranes, with their characteristic caveolae still attached on the side opposite to the silica coating, were incubated for 60 min with cytosol (15) plus GTP at the indicated concentration and repelleted (16). Proteins from these membranes (20 μg) were separated by SDS-polyacrylamide gel electrophoresis (SDS-PAGE) and electrotransferred to nitrocellulose for immunoblotting (8, 14, 17) with antibodies to caveolin, angiotensin converting enzyme (ACE), and 5'-nucleotidase (5'NT). SM, starting material. **(B)** The signals detected in the immunoblots shown in (A) were quantified densitometrically (14, 17) and plotted as a percentage of the signal detected in the starting material and as a function of the GTP concentration. **(C)** The rate of caveolin loss is dependent on the GTP concentration. The silica-coated membranes were treated with the indicated GTP concentration for 0, 5, 15, 60, or 120 min. Caveolin was detected and quantified as in (B) in the repelleted silica-coated membranes. When 100 mM GTP was used (19), the kinetics were almost identical to that shown for 1 mM GTP.

Department of Pathology, Harvard Medical School, Beth Israel Hospital, Research North, 99 Brookline Avenue, Boston, MA 02215, USA.

*To whom correspondence should be addressed. E-mail: jschnitz@bwh.harvard.edu

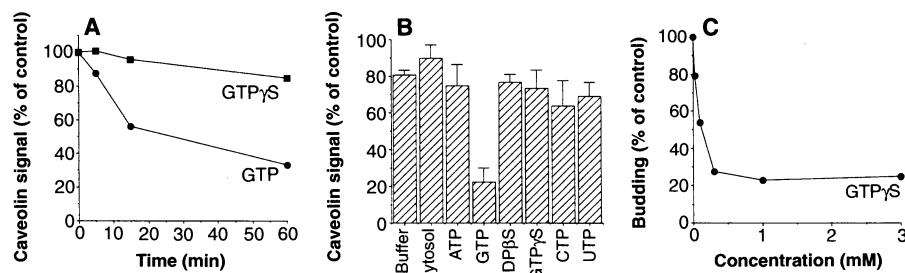


Fig. 2. Requirement of GTP hydrolysis for stimulation of caveolar fission. **(A)** GTP γ S, unlike GTP, does not induce release of caveolin from the silica-coated membranes. The caveolin assay was performed as in Fig. 1 for the indicated times with GTP and GTP γ S at 1 mM. Immunoblot signals for caveolin were quantified densitometrically and plotted as a function of time. **(B)** Various potential effectors were tested for their effects on caveolae budding. The signal for caveolin (quantified relative to the starting material) is shown for the silica-coated membranes repelleted after 60-min treatment with buffer alone, cytosol alone (without ATP), cytosol (with ATP), or cytosol plus ATP supplemented with 1 mM of GTP, GDP β S, GTP γ S, CTP, or UTP as indicated. As would be expected, the membrane processing may in itself disrupt some of the caveolae and cause a small loss in caveolin; in our experiments this loss varied from 0 to 22%. **(C)** GTP γ S competitively prevents GTP stimulation of the budding of caveolae. The caveolae budding assay was performed as in Fig. 1 with 100 μ M GTP in the presence of the indicated concentration of GTP γ S.

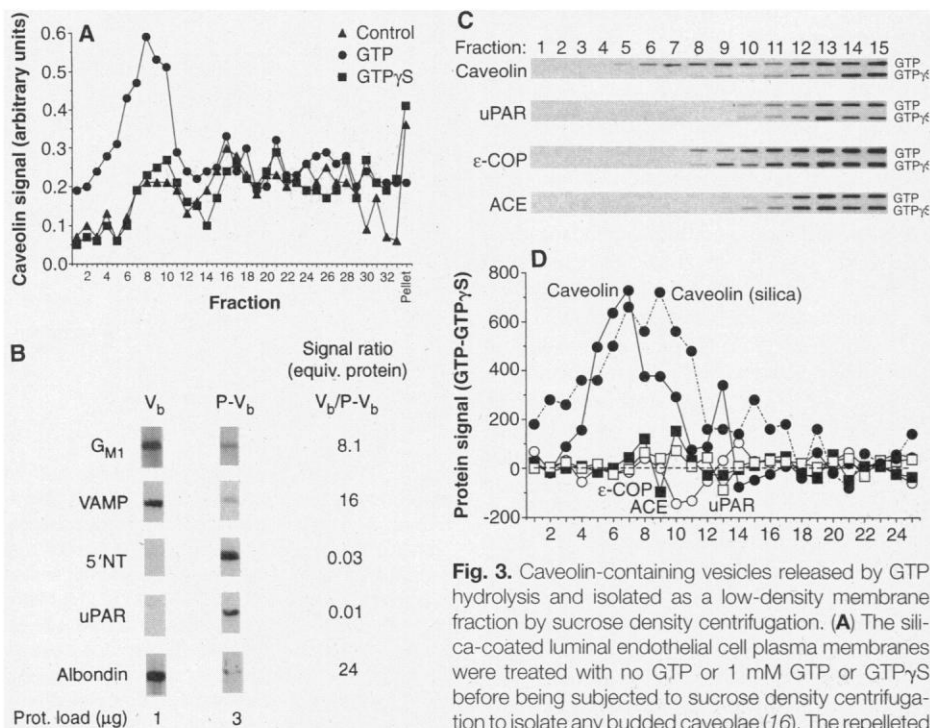


Fig. 3. Caveolin-containing vesicles released by GTP hydrolysis and isolated as a low-density membrane fraction by sucrose density centrifugation. **(A)** The silica-coated luminal endothelial cell plasma membranes were treated with no GTP or 1 mM GTP or GTP γ S before being subjected to sucrose density centrifugation to isolate any budded caveolae (16). The repelleted silica-coated plasma membranes (Pellet) and 33 fractions were collected from the continuous sucrose gradient and processed for enzyme-linked immunosorbent assay (16). The caveolin signal detected for each fraction is plotted. With GTP treatment, plasmalemmal caveolin in the pellet is reduced substantially relative to that for GTP γ S and the control. Caveolin-rich membranes move to the low-density membrane fractions. **(B)** The caveolin-rich budded caveolae in fractions 5 to 10 (V_b) of the sucrose gradient and the membrane pellet (P-V_b) were collected for SDS-PAGE and immunoblotting with the indicated antibodies. **(C)** Caveolin detected in nonsilica-coated plasma membranes treated with GTP or GTP γ S. A plasma membrane-rich fraction isolated from rat lung homogenates by Percoll gradient centrifugation (28) was incubated with cytosol containing 1 mM GTP or GTP γ S for 1 hour at 37°C before sucrose gradient centrifugation as in (A). The buoyant membranes floating into the linear part of the sucrose gradient (top 15 fractions) were analyzed by slot blotting with antibodies to caveolin, ACE, uPAR, and ϵ -COP. Caveolin is detected in the low-density fractions only after GTP treatment, whereas the noncaveolar proteins are not. 5'NT was not detected in the GTP-released low-density caveolin-rich caveolar fractions (19). **(D)** Subtractive densitometric analysis of the sucrose gradient fractions as derived in (A) and (C). The difference between GTP and GTP γ S in the immunosignal detected for the indicated proteins in each fraction was quantified densitometrically. Silica indicates that the silica-coated plasma membranes were used. Data points are the mean of two experiments.

protein VAMP, previously shown to be concentrated in caveolae (17), was enriched in the GTP-budded caveolar vesicles. This finding is consistent with the effect of *N*-ethylmaleimide (NEM) on the NEM-sensitive fusion protein (NSF) in preventing the transcytosis or endocytosis of macromolecules, including albumins (18) and CTB, that bind in caveolae (19). Furthermore, the albumin binding protein albondin (8) was enriched in the budded caveolae, in agreement with the observed transcytosis of albumin via caveolae in endothelium *in situ* (3). Other plasmalemmal molecules [such as the GPI-anchored proteins 5'NT and urokinase-plasminogen activator receptor (uPAR)] were excluded from the budded caveolae, which is consistent with reports that GPI-anchored proteins normally reside in microdomains distinct from caveolae (14, 20) and require perturbants such as antibody cross-linking for sequestration into or near caveolae (21). Thus, caveolae can bud from the cell surface to form discrete carrier vesicles containing a unique subset of plasmalemmal molecules including specific transport molecules.

To exclude the possibility that the silica coating affected our findings, we also examined plasma membranes isolated by Percoll gradient centrifugation (Fig. 3, C and D). The isolated plasmalemmal fraction was rich in the plasma membrane marker ACE and in caveolin (three- to fivefold increase over starting homogenates); however, it was enriched fourfold in the Golgi marker protein ϵ -COP (19, 22). These membranes were treated with GTP or GTP γ S and subjected to sucrose density centrifugation. Slot blotting of the gradient fractions showed that GTP but not GTP γ S induced the specific movement of caveolin-rich membranes away from the heavier bulk membranes into the lower density fractions. These budded caveolae did not contain detectable ACE or GPI-anchored proteins and had a similar density to that of caveolae budding from the silica-coated plasma membranes. It is unlikely that the GTP-released caveolin-rich vesicles were derived from the Golgi membranes contaminating this preparation because the trans-Golgi network exocytic vesicles rich in caveolin also contain abundant GPI-anchored proteins (23).

Next, we confirmed our results from the reconstituted cell-free system by using cultured endothelial cells permeabilized with streptolysin-O (SLO) to allow entry of GTP (24). Again, GTP but not GTP γ S stimulated the budding of caveolae from the cell surface (Fig. 4). Biochemical analysis of the permeabilized bovine lung microvascular endothelial cells (BLMVECs) showed an 80% reduction in plasmalemmal caveolin after GTP but not GTP γ S treatment (Fig. 4A). Electron microscopy analysis (4, 25) confirmed that GTP but

not GTP γ S treatment caused a 78% reduction in the number of caveolae at the surface of these permeabilized cells (Fig. 4B and Table 1).

To verify that these cells, although permeabilized, were functioning normally in caveolar transport, we also examined CTB endocytosis; CTB has been shown in intact cells to bind preferentially within caveolae and accumulate in multivesicular bodies (MVBs) (1). Fluorescence microscopy of the permeabilized BLMVECs (Fig. 4C) showed substantial internalization of cell surface-bound CTB upon warming to 37°C. GTP greatly stimulated CTB endocytosis, causing greater perinuclear accumulation with little labeling remaining at the cell surface. Conversely, GTP γ S inhibited internalization, with CTB being detected only at the cell surface. Electron microscopy revealed that CTB conjugated to gold particles (CTB-Au) was able to enter the caveolae of these permeabilized cells and accumulate inside the cell in MVBs (Fig. 4, D to G). As in intact cells (1), CTB-Au was found inside the bulb of the caveolae and on or near the neck of the caveolae. After only 10 min of warming

to 37°C, CTB-Au was detected in MVBs. It was readily apparent that this endocytosis was greatly stimulated with GTP and inhibited with GTP γ S (Table 1). Only about half of the MVBs in the control cells contained CTB-Au, which increased to more than 90% for GTP-treated cells and decreased to 25% for GTP γ S-treated cells. In addition, with GTP treatment, the number of CTB-Au par-

ticles detected per MVB was 3.5-fold greater than in the control, whereas GTP γ S caused a decrease to one-fifth of the control value.

Thus, it appears that caveolae, in a process requiring GTP hydrolysis, can bud directly from the endothelial cell surface to form discrete carrier vesicles containing the molecular machinery for regulated specific vectorial transport. The formation of secretory and

Table 1. Electron microscopy analysis of the effects of GTP on caveolae and CTB internalization. Permeabilized BLMVECs were treated with cytosol alone or with GTP or GTP γ S as described in the legend to Fig. 4A, before processing for electron microscopy. The cell surface density of caveolae and the internalization of the gold particles were assessed quantitatively as described (4, 25). The number of caveolae per micrometer of plasma membrane was calculated by counting the caveolae in $\geq 140 \mu\text{m}$ of cell surface membrane for each condition. The number of gold particles per MVB was determined for 25 different MVBs in each group. Data are the means \pm SD and the percentages relative to the control.

Treatment	Caveolae density		CTB-Au in MVBs			
	Per μm	% of control	Per MVB	% of control	% MVB-labeled	Range
Control	1.7 \pm 1.1	100	2.1 \pm 2.8	100	48	0 to 7
GTP	0.38 \pm 0.35	22	7.3 \pm 12	351	93	0 to 40
GTP γ S	1.8 \pm 0.57	106	0.42 \pm 0.90	20	25	0 to 4

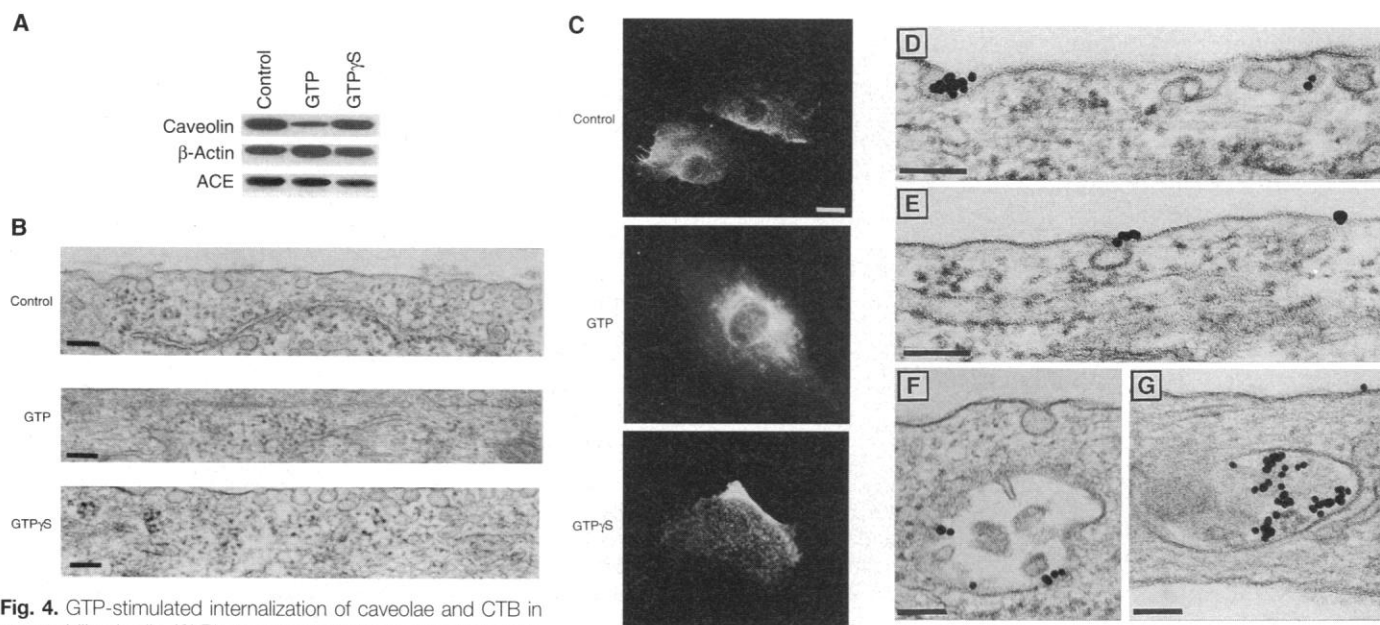


Fig. 4. GTP-stimulated internalization of caveolae and CTB in permeabilized cells. (A) Plasmalemmal caveolin in cultured cells. BLMVECs (4, 8) were permeabilized with SLO (24) before warming to 37°C with the addition of cytosol alone (control) or 1 mM GTP or GTP γ S in cytosol. The cells were coated at 4°C as in (29) with colloidal silica to isolate the silica-coated plasma membranes for SDS-PAGE and immunoblotting with antibodies to caveolin, β -actin, and ACE. An 80% decrease in caveolin was detected after GTP but not GTP γ S treatment of the cells, whereas the amount of ACE and β -actin did not change, consistent with the equal protein loads (20 μg per lane). (B) Electron microscopy. BLMVECs were grown on 35-mm culture dishes as described (4, 8), permeabilized (24), and treated with cytosol alone (control), GTP, or GTP γ S as in (A). After 10 min, the cells were fixed in 3% glutaraldehyde in 0.1 M Na cacodylate (pH 7.4) for 1 hour at 4°C and processed for electron microscopy (4, 25). Representative micrographs are shown of the caveolae detected on the cell surface. Bar, 120 nm. (C) Fluorescence microscopy of CTB processing. CTB conjugated to fluorescein isothiocyanate (5 $\mu\text{g}/\text{ml}$) (Sigma) was bound at 4°C to permeabilized BLMVECs before treatment with cytosol alone (control), GTP, or GTP γ S as in (A). After 10 min the cells were washed, fixed with acetone (-20°C), and processed for photography as described (4, 29). Some CTB endocytosis was evident in the control and was substantially increased by GTP, resulting in little cell surface staining and appreciable perinuclear accumulation. With GTP γ S, CTB remained only at the cell surface (note the lack of nuclear "ghost" image). This cell surface staining is similar to that seen for intact or permeabilized cells maintained at 4°C or after only 1 to 2 min of warm-up to 37°C (19). Bar, 30 μm . (D to G) Electron microscopy of CTB processing by BLMVECs. CTB-Au (optical density at 515 nm = 3.0) prepared as in (14) was bound for 30 min at 4°C to permeabilized BLMVECs, washed, warmed to 37°C with cytosol alone (control) or 1 mM GTP, and then processed for electron microscopy as in (B). (D) Control cell showing gold particles entering caveolae and located in the bulb of the caveolae. (E) Control cell showing gold particles bound at or near the neck of the caveolae. (F) Control cell with gold particles inside the MVB. This was the maximum number of gold particles detected. (G) GTP-treated cell showing large numbers of gold particles accumulating in MVB. Bar, 100 nm.

clathrin-coated endocytic vesicles requires GTP hydrolysis, whereas the budding of endoplasmic reticulum vesicles and COP-coated Golgi vesicles does not and occurs even in the presence of GTP γ S (26, 27). In our cell-free reconstituted assay with the silica-coated plasma membranes, only the latter step (or steps) in the formation of free vesicles can be examined, because the firmly attached silica-coating prevents movement so that new invaginations cannot readily form. Hence, in this assay GTP has stimulated the fission of caveolar invaginations to complete the budding process and create free caveolar vesicles. Because GTP does not stimulate budding in the absence of cytosol (19), a specific cytosolic factor (or factors), possibly a guanosine triphosphatase (GTPase), may bind to the caveolae to permit fission. Endothelial cell caveolae have been found to contain various GTPases bound to the membrane (17). Further definition of the molecular mechanisms mediating budding remains a challenge for the future.

REFERENCES AND NOTES

1. R. Montesano, J. Roth, A. Robert, L. Orci, *Nature* **296**, 651 (1982); D. Trans, J.-L. Carpentier, F. Sawano, P. Gorden, L. Orci, *Proc. Natl. Acad. Sci. U.S.A.* **84**, 7957 (1987); R. G. Parton, *J. Histochem. Cytochem.* **42**, 155 (1994).
2. C. Huet, J. F. Ash, S. J. Singer, *Cell* **21**, 429 (1980); G. Raposo et al., *Eur. J. Cell Biol.* **50**, 340 (1989); R. I. Goldberg, R. M. Smith, L. Jarett, *J. Cell Physiol.* **133**, 203 (1987); G. E. Palade and R. R. Bruns, *J. Cell Biol.* **37**, 633 (1968); L. Ghitescu, A. Fixman, M. Simionescu, N. Simionescu, *ibid.* **102**, 1304 (1986).
3. A. J. Millici, N. E. Watrous, H. Stukenbrok, G. E. Palade, *J. Cell Biol.* **105**, 2603 (1987); L. Ghitescu and M. Bendayan, *ibid.* **117**, 745 (1992).
4. J. E. Schnitzer, P. Oh, E. Pinney, A. Allard, *ibid.* **127**, 1217 (1994).
5. R. G. Parton, B. Joggerst, K. Simons, *ibid.*, p. 1199.
6. G. L. King and S. M. Johnson, *Science* **227**, 1583 (1985).
7. J. E. Schnitzer, *Trends Cardiovasc. Med.* **3**, 1024 (1993).
8. _____ and P. Oh, *J. Biol. Chem.* **269**, 6072 (1994); *Am. J. Physiol.* **263**, H1872 (1992).
9. J. E. Schnitzer, A. Sung, R. Horvat, J. Bravo, *J. Biol. Chem.* **264**, 24544 (1992); J. E. Schnitzer and J. Bravo, *ibid.* **268**, 7562 (1993).
10. E. J. Smart, D. C. Foster, Y.-S. Ying, B. A. Kamen, R. G. W. Anderson, *J. Cell Biol.* **124**, 307 (1994).
11. N. J. Severs, *J. Cell Sci.* **90**, 341 (1988); B. Van Deurs, P. K. Holm, K. Sandvig, S. H. Hansen, *Trends Cell Biol.* **3**, 249 (1993).
12. M. Bundgaard, J. Frokjaer-Jensen, C. Crone, *Proc. Natl. Acad. Sci. U.S.A.* **76**, 6439 (1979); J. Frokjaer-Jensen, *J. Ultrastruct. Res.* **73**, 9 (1980); M. Bundgaard, *Fed. Proc.* **42**, 2425 (1983); J. Frokjaer-Jensen, R. C. Wagner, S. B. Andrews, P. Hagman, T. S. Reese, *Cell Tissue Res.* **254**, 17 (1988); J. J. Frokjaer-Jensen, *J. Electron Microsc. Tech.* **19**, 291 (1991).
13. K. G. Rothberg, Y. Ying, J. F. Kolhouse, B. A. Kamen, R. G. W. Anderson, *J. Cell Biol.* **110**, 637 (1990); R. G. W. Anderson, B. A. Kamen, K. G. Rothberg, S. W. Lacey, *Science* **255**, 410 (1992).
14. J. E. Schnitzer, D. P. McIntosh, A. M. Dvorak, J. Liu, P. Oh, *Science* **269**, 1435 (1995); J. E. Schnitzer, P. Oh, B. S. Jacobson, A. M. Dvorak, *Proc. Natl. Acad. Sci. U.S.A.* **92**, 1759 (1995).
15. Cytosol was isolated from rat lungs perfused as described (8, 14). The lungs were flushed free of blood, perfused with cold protease inhibitors, and homogenized in ice-cold cytosolic buffer (2 \times v/w) (25 mM KCl, 2.5 mM Mg acetate, 5 mM EGTA, 150 mM K acetate, and 25 mM Hepes titrated to a final pH of 7.4 with KOH). The homogenate was centrifuged at 100,000g for 1 hour at 4°C, and the supernatant was collected. This cytosol was filtered with a prepacked DG-10 column (Bio-Rad), and samples were stored frozen at -80°C. Unless indicated otherwise, the filtered cytosol (final concentration, 5 mg/ml) was supplemented just before experimentation with 2 mM ATP and an ATP-regeneration system of creatine phosphokinase (16.7 U/ml) and 16.7 mM phosphocreatine.
16. A cell-free assay for caveolar fission was reconstituted with the silica-coated luminal endothelial cell plasma membranes purified from rat lungs as described (14). The silica-coated membranes were mixed gently for 0 to 120 min at 37°C with cytosol (15) containing 1 mM GTP (unless indicated otherwise) before the addition of ice-cold 60% sucrose in 20 mM KCl to achieve a final 30% sucrose concentration. The mixture was layered onto a cushion of 40% sucrose in a SW55 centrifuge tube, and then 20% sucrose was added to the tube before topping with 20 mM KCl. After centrifugation for 2 hours (30,000 rpm in a SW55 rotor) at 4°C, the pellet containing the silica-coated membranes was processed for immunoblot analysis and densitometric quantification of the signal as described (14, 17). For isolation of released caveolae, the membranes were treated as above with 1 mM GTP for 60 min, except that centrifugation was performed with a continuous sucrose gradient as described (15).
17. J. E. Schnitzer, J. Liu, P. Oh, *J. Biol. Chem.* **270**, 14399 (1995).
18. J. E. Schnitzer, P. Oh, E. Pinney, J. Allard, *Am. J. Physiol.* **268**, H48 (1995); D. Predescu, R. Horvat, S. Predescu, G. E. Palade, *Proc. Natl. Acad. Sci. U.S.A.* **91**, 3014 (1994).
19. J. E. Schnitzer, P. Oh, D. P. McIntosh, unpublished data.
20. A. M. Fra, E. Williamson, K. Simons, R. G. Parton *J. Biol. Chem.* **269**, 30745 (1994); A. Gorodinsky and D. A. Harris *J. Cell Biol.* **129**, 619 (1995).
21. S. Mayor, K. G. Rothberg, F. R. Maxfield, *Science* **264**, 1948 (1994).
22. The purified silica-coated plasma membranes did not contain detectable ϵ -COP or other intracellular organelle markers (14, 19).
23. T. V. Kurzchalia et al., *J. Cell Biol.* **118**, 1003 (1992); P. Dupree, R. G. Parton, G. Raposo, T. V. Kurzchalia, K. Simons, *EMBO J.* **12**, 1597 (1993); D. Brown and J. K. Rose, *Cell* **68**, 533 (1992).
24. For permeabilization, the cells were cooled to 4°C for 10 min and washed once with ice-cold buffer A [20 mM Hepes, 110 mM NaCl, 2 mM CaCl₂, 5.4 mM KCl, 0.9 mM Na₂HPO₄, 10 mM MgCl₂, 11 mM glucose (pH 7.4)]. Reduced SLO dissolved in buffer A at 0.6 U/ml was bound at 4°C for 10 min before washing twice in ice-cold buffer A and incubation in buffer A at 37°C for 15 min to induce pore formation in the plasma membranes.
25. J. E. Schnitzer, A. Siflinger-Birboim, P. J. Del Vecchio, A. B. Malik, *Biochem. Biophys. Res. Commun.* **199**, 11 (1994).
26. S. A. Tooze, U. Weiss, W. B. Huttner, *Nature* **347**, 207 (1990); M. F. Rexach and R. W. Schekman, *J. Cell Biol.* **114**, 219 (1991); L. L. Carter, T. E. Reddelmeier, L. A. Woolenweber, S. L. Schmid, *ibid.* **120**, 37 (1993).
27. V. Maholtra, T. Serafini, L. Orci, J. C. Shepherd, J. E. Rothman, *Cell* **58**, 329 (1989); R. Schwaninger, H. Plutner, G. M. Bokoch, W. E. Balch, *J. Cell Biol.* **119**, 1077 (1992).
28. E. J. Smart, Y.-S. Ying, C. Mineo, R. W. G. Anderson, *Proc. Natl. Acad. Sci. U.S.A.* **92**, 10104 (1995).
29. J. E. Schnitzer and P. Oh, *Am. J. Physiol.* **270**, 416 (1996).
30. We are indebted to R. Jahn, R. A. Skidgel, M. Krieger, and J. P. Luzio for supplying antibodies to VAMP, ACE, ϵ -COP, and 5'NT, respectively. Supported by the Beth Israel Hospital Foundation, a Grant-in-Aid from the American Heart Association, and NIH grants HL43278 and HL52766 (J.E.S.). Work for this study was carried out during the tenure of an Established Investigator Award from the American Heart Association and Genentech (J.E.S.).

24 July 1996; accepted 20 August 1996

Association of Spindle Assembly Checkpoint Component X_{MAD2} with Unattached Kinetochores

Rey-Huei Chen, Jennifer C. Waters, E. D. Salmon, Andrew W. Murray*

The spindle assembly checkpoint delays anaphase until all chromosomes are attached to a mitotic spindle. The *mad* (mitotic arrest-deficient) and *bub* (budding uninhibited by benzimidazole) mutants of budding yeast lack this checkpoint and fail to arrest the cell cycle when microtubules are depolymerized. A frog homolog of *MAD2* (*X_{MAD2}*) was isolated and found to play an essential role in the spindle assembly checkpoint in frog egg extracts. *X_{MAD2}* protein associated with unattached kinetochores in prometaphase and in nocodazole-treated cells and disappeared from kinetochores at metaphase in untreated cells, suggesting that *X_{MAD2}* plays a role in the activation of the checkpoint by unattached kinetochores. This study furthers understanding of the mechanism of cell cycle checkpoints in metazoa and provides a marker for studying the role of the spindle assembly checkpoint in the genetic instability of tumors.

The cell division cycle is a highly ordered and tightly regulated process. Its transitions are monitored by checkpoints that delay the cell cycle until critical events are completed (1-3). Accurate chromosome segregation requires that chromosomes attach to

and become aligned on the mitotic spindle before activation of the cyclin proteolysis machinery induces sister chromatid separation, cyclin B degradation, and loss of histone H1 kinase activity of p34^{cdc2}. Inhibition of spindle assembly with microtubule